# Temperature Effects in the Band Structure of Topological Insulators

Bartomeu Monserrat[1,2,*] and David Vanderbilt[1]
[1]Department of Physics and Astronomy, Rutgers University, Piscataway, New Jersey 08854-8019, USA
[2]TCM Group, Cavendish Laboratory, University of Cambridge, J. J. Thomson Avenue, Cambridge CB3 0HE, United Kingdom
(Received 3 August 2016; revised manuscript received 23 September 2016; published 22 November 2016)

We study the effects of temperature on the band structure of the $Bi_2Se_3$ family of topological insulators using first-principles methods. Increasing temperature drives these materials towards the normal state, with similar contributions from thermal expansion and from electron-phonon coupling. The band gap changes with temperature reach 0.3 eV at 600 K, of similar size to the changes caused by electron correlation. Our results suggest that temperature-induced topological phase transitions should be observable near critical points of other external parameters.

DOI: 10.1103/PhysRevLett.117.226801

Topological insulators and related materials have consolidated as a new field of condensed matter of both fundamental and applied interest. Potentially novel applications have motivated the search for new materials exhibiting topological properties. In this quest, composition [1], pressure [2,3], strain [4,5], and electromagnetic fields [6–8] have all been used to control topological order. By contrast, temperature has so far exclusively played a passive role, for example, constraining the quantum anomalous Hall effect to the milikelvin regime [9], and thus limiting potential applications of the associated dissipationless currents. Only recently have Saha and coworkers proposed that temperature can also be exploited when studying topological materials, for example, by using phonon linewidths to identify band inversions [10].

The effects of temperature on topological insulators can be divided into two areas. The first concerns the electronic occupation of states, leading to questions such as the proper definition of topological invariants, which must then be based on the density matrix rather than the ground state wave function [11–14]. The second relates to the renormalization of the single-particle bands, which could lead to temperature-induced band inversions [15,16], and it has been argued on the basis of simple models that temperature should favor topological phases.

First-principles calculations have proved central in predicting new topological materials and their behavior, many times leading to subsequent experimental observation [17,18]. The study of temperature effects on topological materials would equally benefit from first-principles calculations, but none have been available. Fully first-principles calculations of the temperature dependence of band structures have only recently become possible, as first and second order terms in the electron-phonon interaction contribute similarly and must be included on an equal footing [19,20]. Because of such difficulties, to date these calculations have only been performed on simple semiconductors and insulators [21–25]. To use these techniques for topological materials, they need to be extended to include the effects of spin-orbit coupling in the calculation of the electron-phonon interaction.

In this work, we study the effects of temperature on topological insulators with first-principles methods. Using the $Bi_2Se_3$ family of topological insulators, we demonstrate the feasibility of such calculations and unravel the importance of temperature when studying topological order. Our calculations show that both thermal expansion and electron-phonon coupling make similar contributions to the temperature dependence of band structures, and that, at variance with predictions from model studies [15,16], increased temperature tends to suppress topological order in these materials.

We consider the $Bi_2Se_3$ family of compounds for our first-principles study [17]. $Bi_2Te_3$, $Bi_2Se_3$, and $Sb_2Te_3$ crystallize in the rhombohedral $R\bar{3}m$ space group, with five atoms in the primitive cell. They form a layered structure, in which groups of five layers are tightly bound (so-called quintuple layers), and these are then weakly bound to each other. $Sb_2Se_3$ has $Pnma$ symmetry in its ground state. Metastable structures of these compounds have been synthesized [26], and, in particular, the $R\bar{3}m$ structure of $Sb_2Se_3$ has been experimentally studied [3]. In this work, we consider the $R\bar{3}m$ structure for all compounds.

Our calculations are based on density functional theory (DFT) using the VASP package [27–30]. We use the PBE functional [31] and the projector augmented-wave method [32,33] with an energy cutoff of 600 eV and a $\mathbf{k}$-point grid of size $12 \times 12 \times 12$ for the primitive cells and commensurate grids for the supercells. All calculations are performed with spin-orbit coupling unless otherwise stated.

The PBE functional overestimates static volumes and thermal expansion compared to experiment. For example, in $Bi_2Se_3$ the experimental hexagonal $c$ axis at 10 K is 28.48 Å [34], compared with the PBE $c$ axis of 30.21 Å. Therefore, we use experimental volumes when available. For $Bi_2Se_3$ and $Sb_2Te_3$, experimental data is only available

 

up to about 250 K [34], and we fit a Bose factor to this data to extrapolate to higher temperatures, which is justified in this case as the linear asymptotic regime is already reached at the highest temperatures for which data are available [35]. For $Bi_2Te_3$, data are available up to 600 K [36]. No data are available for the rhombohedral structure of $Sb_2Se_3$, so in this case we use the structure relaxed using the PBE functional. The atomic coordinates of all atoms are relaxed until the forces are smaller than $10^{-3}$ eV/Å.

The phonon and electron-phonon coupling calculations are performed using the finite displacement method in conjunction with the recently developed nondiagonal supercell approach [37]. Finite displacement methods allow us to straightforwardly incorporate the effects of the spin-orbit interaction on electron-phonon coupling which, as far as we are aware, has never been attempted in this context. The reported results correspond to a vibrational Brillouin zone sampling using grid sizes of $4 \times 4 \times 4$. The matrix of force constants is constructed by considering small positive and negative symmetry-inequivalent atomic displacements of amplitude 0.005 Å. The dynamical matrix, obtained by a Fourier transformation, is diagonalized to calculate the vibrational frequencies $\omega_{\mathbf{q}\nu}$ at each phonon wave vector $\mathbf{q}$ and branch $\nu$. The band gap at temperature $T$ is then calculated as [19–25]

$$E_g(T) = E_g^{\text{static}} + \frac{1}{N_{\mathbf{q}}} \sum_{\mathbf{q},\nu} \frac{a_{\mathbf{q}\nu}}{\omega_{\mathbf{q}\nu}} \left[ \frac{1}{2} + n_B(\omega_{\mathbf{q}\nu}, T) \right], \quad (1)$$

where $a_{\mathbf{q}\nu}$ are the electron-phonon matrix elements averaged over $N_{\mathbf{q}}$ $\mathbf{q}$ points, and $n_B$ is a Bose-Einstein factor. The electron-phonon matrix elements are determined using finite displacements along the normal modes of vibration. To test the accuracy of our calculations, we evaluate Eq. (1) for $Bi_2Se_3$ using grids of size $8 \times 8 \times 8$, and find that the maximum change in the electron-phonon induced band gap corrections is only 8 meV at all temperatures considered. Electron-phonon coupling calculations using Monte Carlo integration, which allow us to assess the importance of higher-order terms in the electron-phonon coupling interaction, show that higher-order terms are negligible at zero temperature, and while their contribution increases with increasing temperature, the conclusions of the Letter are not affected by them.

The topological nature of the $Bi_2Se_3$ family of compounds is determined by the parity of the occupied bands at the Γ point, where band inversion occurs in the presence of spin-orbit coupling [17]. Therefore, in order to investigate the effects of temperature on the topological order, we focus on the temperature dependence of the band gap at Γ, as shown in Fig. 1.

$Bi_2Te_3$, $Bi_2Se_3$, and $Sb_2Te_3$ are topological insulators, and their gaps decrease with increasing temperature. Using $Bi_2Se_3$ as an example, we observe that the gap reduction is driven by both thermal expansion and electron-phonon coupling. Thermal expansion alone (orange dashed line) decreases the band gap by almost 0.1 eV at 600 K. Electron-phonon coupling alone (blue dashed-dotted line) causes a change in the band gap of 0.1 eV at 600 K. The asymptotic linear dependence of the gap change with temperature is reached at around 100 K, determined by the low-energy vibrations that are a consequence of the heavy atoms in the compounds under study. Thermal expansion and electron-phonon coupling make similar contributions, and therefore both must be included (red solid line). To date, the vast majority of first-principles calculations of the temperature dependence of the band gap have neglected the effects of thermal expansion. This may be justifiable for simple materials made of light atoms, such as diamond and silicon, that exhibit weak thermal expansion. By contrast, topological insulators are composed of heavy elements, for which thermal expansion is important as shown in Fig. 1.

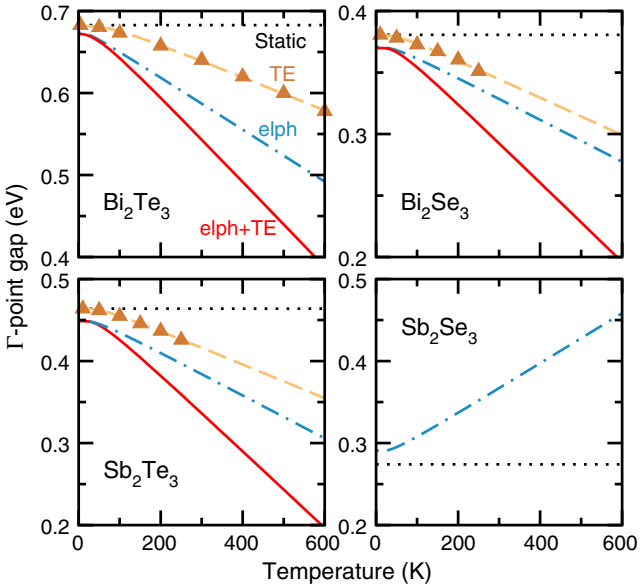


FIG. 1. Temperature dependence of the Γ-point band gaps of the $Bi_2Se_3$ family of compounds. The black dotted lines correspond to the static lattice band gaps; the orange dashed and blue dashed-dotted lines show the result of including only thermal expansion or only electron-phonon coupling effects, respectively; the red solid curves give the total temperature dependence.

Not surprisingly, for $Sb_2Se_3$, which is already a normal insulator with an uninverted gap at low temperature, the same electron-phonon effects lead instead to an increase of the band gap with increasing temperature. Thermal expansion also tends to increase the band gap, but we have not included this contribution as there is no experimental data available for this system.

The direct band gaps at the Γ point are not the minimum band gaps in $Bi_2Te_3$ and $Sb_2Te_3$. We also investigate the temperature dependence of the minimum band gaps of these two materials, and we find that the band gap grows with increasing temperature, and the band gap changes are smaller

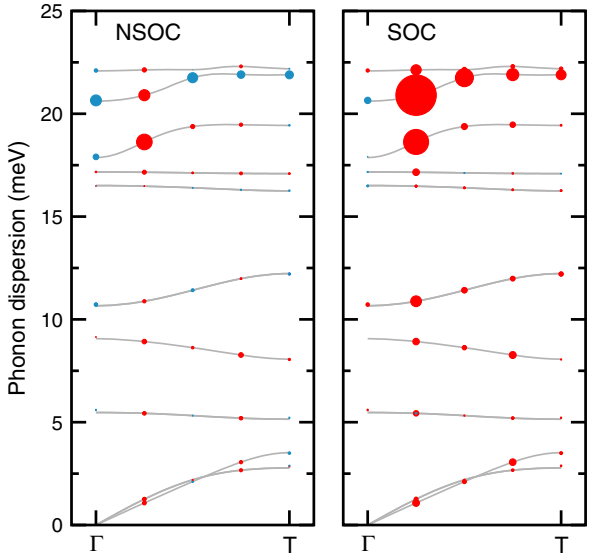


FIG. 2. Phonon dispersion of $Bi_2Se_3$ with mode resolved electron-phonon coupling strength without (left) and with (right) spin-orbit coupling. The area of the circles are proportional to the strength of electron-phonon coupling, and the sign of the coupling is positive (widening the gap) for blue circles and negative (reducing the gap) for red circles.

than those observed for the Γ point gaps. Further details of these calculations are provided in the Supplemental Material [38].

The sizes of the band gap shifts are similar to those observed and calculated in many semiconductors and insulators. The only reported phonon-induced gap shifts in topological insulators we are aware of are those of Kim and Jhi, who theoretically studied the change in the band gap induced by exciting selected phonon modes in a series of IV-VI semiconductors and found shifts on the 0.1 eV scale [39]. In the $Bi_2Se_3$ family of compounds, zero-point contributions are small, in the range 0.01–0.02 eV in all systems, but thermal changes are larger, reaching 0.2–0.3 eV at 600 K. The *GW* approximation has been shown to correct the DFT gaps by about 0.2–0.3 eV in the $Bi_2Se_3$ family of compounds [40], to lead to qualitative changes in the shape of the bands near Γ [41], and, more generally, to question the validity of some predictions of topological insulators based on semilocal DFT [42]. Our results show that the effects of temperature modify the band structure to a similar extent, and, therefore, should also be included for an accurate description of topological insulators.

We next investigate the microscopic origin of the electron-phonon coupling strength, taking $Bi_2Se_3$ as an example. In Fig. 2 we show the phonon dispersion of $Bi_2Se_3$ along the high-symmetry line from Γ at $\mathbf{q} = (0, 0, 0)$ to $T$ at $\mathbf{q} = (0.5, 0.5, 0.5)$, chosen because electron-phonon coupling is strongest along this line. The mode-resolved strength of electron-phonon coupling to the direct band gap at the electronic Γ point is indicated by the filled circles, and shown both without and with spin-orbit coupling. The inclusion of the spin-orbit interaction has two effects. The first is to reverse the band gap increase induced by electron-phonon coupling to band gap reduction upon band inversion. The second is to modify the strength of electron-phonon coupling beyond the mere exchange of band extrema. For example, the gap reduction induced by the modes at $\mathbf{q} = (0.25, 0.25, 0.25)$ with spin-orbit coupling is larger than the increase of the gap induced by the same modes when spin-orbit coupling is not included. For $Bi_2Te_3$ and $Sb_2Te_3$, similar behavior is observed, but for $Sb_2Se_3$, the inclusion of spin-orbit coupling does not induce a band inversion, and, therefore, the sign of the band gap correction does not reverse.

A detailed analysis of the couplings reveals that the modes that couple most strongly to the electronic states are those that involve atomic vibrations along the $c$ axis that change the interlayer distance. It is also the change in length of the $c$ axis that drives the band gap change due to thermal expansion. This can be explained by the nature of the states at the band extrema of the Γ point, which mainly arise from the hybridized $p$ orbitals of the constituent atoms. The crystal field splits the $p_z$ from the $p_{x,y}$ orbitals, which remain degenerate, and it is the $p_z$ that form the band extrema and undergo band inversion when the spin-orbit interaction is included [17]. Changing the interlayer distance, either by atomic vibrations or by lattice expansion, modifies the states at the gap edges, and thus drives the observed temperature dependence.

Overall, the results reported in Fig. 1 show that no band closure occurs in any of the four materials studied as a function of temperature. As a consequence, the $Z_2$ indices of these materials calculated at the static lattice level do not change with temperature.

The inclusion of temperature in our calculations allows us to construct the pressure-temperature phase diagram of $Sb_2Se_3$ shown in Fig. 3. $Sb_2Se_3$ is a normal insulator under ambient pressure, but with increasing external pressure it undergoes a phase transition to a topological insulator at 2.5 GPa [3]. First-principles calculations based on the PBE functional give a transition pressure of 1.0 GPa [43]. Our own calculations using PBE give a similar transition pressure of 0.5 GPa, and we also perform HSE calculations [44,45], which increase the transition pressure to 2.5 GPa, in better agreement with experiment. Because of the computational cost of HSE calculations, we perform the finite temperature calculations using the PBE functional instead, and we expect that our results will be qualitatively correct. Figure 3 shows that, with increasing temperature and for pressures above 0.5 GPa, a band gap closure occurs. The parity-analysis based $Z_2$ indices for the static lattices show that the system is a normal insulator at pressures below 0.5 GPa and a topological insulator at higher pressures. Since the band gap only closes along the phase boundary shown in Fig. 3, and since topological character cannot change without a gap closure, we can use continuity

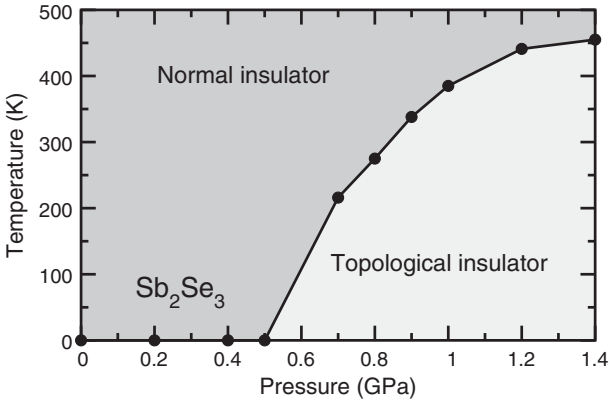


FIG. 3. Pressure-temperature phase diagram of $Sb_2Se_3$. Experimentally, the pressure-induced phase transition is observed at 2.5 GPa [3].

to assign the normal and topological phases as shown in the figure. The pressure-temperature phase diagrams of $Bi_2Te_3$, $Bi_2Se_3$, and $Sb_2Te_3$ are qualitatively similar to that of $Sb_2Se_3$. These materials, however, are deep inside the topological part of the phase diagram at ambient pressure so that unrealistically high temperatures would be needed to induce a transition to the normal state (see Fig. 1).

Experimental observation of a temperature-induced topological phase transition in $Sb_2Se_3$ should be simplest at pressures just above the zero-temperature transition pressure, which experimentally is observed around 2.5 GPa [3]. More generally, temperature-induced topological phase transitions should be observable near critical values of other external parameters driving a topological phase transition. A phase diagram similar to our prediction in Fig. 3 has been recently reported in experiments on (Pb,Sn)Se [46].

Our results show that in the $Bi_2Se_3$ family of compounds, increasing temperature favors the normal phase. This is at odds with the theoretical prediction of Refs. [15,16], where it was argued that higher temperature should favor topological phases. The focus there is on electron-phonon coupling only, but we have shown that thermal expansion is equally important. Even if only electron-phonon coupling is considered, our calculations still show that temperature does not favor topological phases in the $Bi_2Se_3$ family of compounds. To understand the discrepancy, we note several possibilities. First, the analysis of Refs. [15,16] only includes the so-called Fan term, which arises from treating the first-order phonon-induced change in the Hamiltonian at second order in perturbation theory. However, the Debye-Waller term, which arises from the second-order change in the Hamiltonian treated at first order in perturbation theory, has been shown to be equally important for the calculation of the temperature dependence of band gaps [21]. Our finite displacement approach includes both terms. Second, the analysis of Refs. [15,16] assumes that the two bands that participate in the band inversion are well separated in energy from the rest of the bands. This ensures that, for sufficiently small gaps, the dominant contribution comes from intraband transitions, which tend to increase the size of the gap in topological insulators. In the systems we have studied, the bands at $\Gamma$ involved in the band inversion are not well separated in energy from other bands. For example, the conduction band minimum of $Bi_2Te_3$ and $Sb_2Te_3$ is not even at $\Gamma$, where band inversion occurs. Therefore, we do not expect that the analysis of Refs. [15,16] applies in our case. Nonetheless, there is no reason why temperature could not favor topological order in some other materials that obey the assumptions laid out in Refs. [15,16], and it would certainly be interesting to identify some such examples.

In summary, we have shown that thermal expansion and electron-phonon coupling drive the temperature dependence of the band structure of topological insulators. Increasing temperature favors the normal state in the $Bi_2Se_3$ family of compounds, and induces a topological phase transition in pressurized $Sb_2Se_3$. Temperature-induced changes to the band gaps reach 0.3 eV at 600 K, and are of similar size to the changes induced by electron correlation in these materials. Open questions remain, such as the effects of thermally induced changes in electron occupation, and the possible importance of nonadiabatic phenomena, especially close to band inversions.

Our work shows that first-principles calculations of the effects of temperature on topological materials are feasible, and that temperature can have important effects on the band structure and topological order of these materials. It should facilitate future work, for example in the search for a room-temperature Chern insulator.

We thank Xavier Gonze for valuable discussions. This work was funded by NSF Grant No. DMR-1408838. B. M. thanks Robinson College, Cambridge, and the Cambridge Philosophical Society for a Henslow Research Fellowship.

*Note added.*—Antonius and Louie recently reported first-principles calculations of the temperature dependence of the band structure of the topological insulator $BiTl(S_{1-\delta}Se_\delta)_2$ [47].

*monserrat@physics.rutgers.edu

[1] D. Hsieh, D. Qian, L. Wray, Y. Xia, Y. S. Hor, R. J. Cava, and M. Z. Hasan, A topological Dirac insulator in a quantum spin Hall phase, Nature (London) **452**, 970 (2008).

[2] X. Xi, C. Ma, Z. Liu, Z. Chen, W. Ku, H. Berger, C. Martin, D. B. Tanner, and G. L. Carr, Signatures of a Pressure-Induced Topological Quantum Phase Transition in BiTeI, Phys. Rev. Lett. **111**, 155701 (2013).

[3] A. Bera, K. Pal, D. V. S. Muthu, S. Sen, P. Guptasarma, U. V. Waghmare, and A. K. Sood, Sharp Raman Anomalies and Broken Adiabaticity at a Pressure Induced Transition from Band to Topological Insulator in $Sb_2Se_3$, Phys. Rev. Lett. **110**, 107401 (2013).

[4] Y. Liu, Y. Y. Li, S. Rajput, D. Gilks, L. Lari, P. L. Galindo, M. Weinert, V. K. Lazarov, and L. Li, Tuning Dirac states by strain in the topological insulator $Bi_2Se_3$, Nat. Phys. **10**, 294 (2014).

[5] S. Liu, Y. Kim, L. Z. Tan, and A. M. Rappe, Strain-induced ferroelectric topological insulator, Nano Lett. **16**, 1663 (2016).

[6] M. Kim, C. H. Kim, H.-S. Kim, and J. Ihm, Topological quantum phase transitions driven by external electric fields in $Sb_2Te_3$ thin films, Proc. Natl. Acad. Sci. U.S.A. **109**, 671 (2012).

[7] T. Zhang, J. Ha, N. Levy, Y. Kuk, and J. Stroscio, Electric-Field Tuning of the Surface Band Structure of Topological Insulator $Sb_2Te_3$ Thin Films, Phys. Rev. Lett. **111**, 056803 (2013).

[8] Q. Liu, X. Zhang, L. B. Abdalla, A. Fazzio, and A. Zunger, Switching a normal insulator into a topological insulator via electric field with application to phosphorene, Nano Lett. **15**, 1222 (2015).

[9] C.-Z. Chang *et al.*, Experimental observation of the quantum anomalous Hall effect in a magnetic topological insulator, Science **340**, 167 (2013).

[10] K. Saha, K. Légaré, and I. Garate, Detecting Band Inversions by Measuring the Environment: Fingerprints of Electronic Band Topology in Bulk Phonon Linewidths, Phys. Rev. Lett. **115**, 176405 (2015).

[11] O. Viyuela, A. Rivas, and M. A. Martin-Delgado, Uhlmann Phase as a Topological Measure for One-Dimensional Fermion Systems, Phys. Rev. Lett. **112**, 130401 (2014).

[12] Z. Huang and D. P. Arovas, Topological Indices for Open and Thermal Systems via Uhlmann's Phase, Phys. Rev. Lett. **113**, 076407 (2014).

[13] O. Viyuela, A. Rivas, and M. A. Martin-Delgado, Two-Dimensional Density-Matrix Topological Fermionic Phases: Topological Uhlmann Numbers, Phys. Rev. Lett. **113**, 076408 (2014).

[14] J. C. Budich and S. Diehl, Topology of density matrices, Phys. Rev. B **91**, 165140 (2015).

[15] I. Garate, Phonon-Induced Topological Transitions and Crossovers in Dirac Materials, Phys. Rev. Lett. **110**, 046402 (2013).

[16] K. Saha and I. Garate, Phonon-induced topological insulation, Phys. Rev. B **89**, 205103 (2014).

[17] H. Zhang, C.-X. Liu, X.-L. Qi, X. Dai, Z. Fang, and S.-C. Zhang, Topological insulators in $Bi_2Se_3$, $Bi_2Te_3$ and $Sb_2Te_3$ with a single Dirac cone on the surface, Nat. Phys. **5**, 438 (2009).

[18] A. A. Soluyanov, D. Gresch, Z. Wang, Q. Wu, M. Troyer, X. Dai, and B. Andrei Bernevig, Type-II Weyl semimetals, Nature (London) **527**, 495 (2015).

[19] P. B. Allen and V. Heine, Theory of the temperature dependence of electronic band structures, J. Phys. C **9**, 2305 (1976).

[20] F. Giustino, Electron-phonon interactions from first principles, arXiv:1603.06965 [Rev. Mod. Phys. (to be published)].

[21] F. Giustino, S. G. Louie, and M. L. Cohen, Electron-Phonon Renormalization of the Direct Band Gap of Diamond, Phys. Rev. Lett. **105**, 265501 (2010).

[22] E. Cannuccia and A. Marini, Effect of the Quantum Zero-Point Atomic Motion on the Optical and Electronic Properties of Diamond and Trans-Polyacetylene, Phys. Rev. Lett. **107**, 255501 (2011).

[23] C. E. Patrick and F. Giustino, Quantum nuclear dynamics in the photophysics of diamondoids, Nat. Commun. **4**, 2006 (2013).

[24] B. Monserrat and R. J. Needs, Comparing electron-phonon coupling strength in diamond, silicon, and silicon carbide: First-principles study, Phys. Rev. B **89**, 214304 (2014).

[25] S. Poncé, G. Antonius, P. Boulanger, E. Cannuccia, A. Marini, M. Côté, and X. Gonze, Verification of first-principles codes: Comparison of total energies, phonon frequencies, electron-phonon coupling and zero-point motion correction to the gap between ABINIT and QE/Yambo, Comput. Mater. Sci. **83**, 341 (2014).

[26] J. Zhao, H. Liu, L. Ehm, D. Dong, Z. Chen, and G. Gu, High-pressure phase transitions, amorphization, and crystallization behaviors in $Bi_2Se_3$, J. Phys. Condens. Matter **25**, 125602 (2013).

[27] G. Kresse and J. Hafner, Ab initio molecular dynamics for liquid metals, Phys. Rev. B **47**, 558 (1993).

[28] G. Kresse and J. Hafner, Ab initio molecular-dynamics simulation of the liquid-metal-amorphous-semiconductor transition in germanium, Phys. Rev. B **49**, 14251 (1994).

[29] G. Kresse and J. Furthmüller, Efficiency of ab-initio total energy calculations for metals and semiconductors using a plane-wave basis set, Comput. Mater. Sci. **6**, 15 (1996).

[30] G. Kresse and J. Furthmüller, Efficient iterative schemes for ab initio total-energy calculations using a plane-wave basis set, Phys. Rev. B **54**, 11169 (1996).

[31] J. P. Perdew, K. Burke, and M. Ernzerhof, Generalized Gradient Approximation Made Simple, Phys. Rev. Lett. **77**, 3865 (1996).

[32] P. E. Blöchl, Projector augmented-wave method, Phys. Rev. B **50**, 17953 (1994).

[33] G. Kresse and D. Joubert, From ultrasoft pseudopotentials to the projector augmented-wave method, Phys. Rev. B **59**, 1758 (1999).

[34] X. Chen, H. D. Zhou, A. Kiswandhi, I. Miotkowski, Y. P. Chen, P. A. Sharma, A. L. Lima Sharma, M. A. Hekmaty, D. Smirnov, and Z. Jiang, Thermal expansion coefficients of $Bi_2Se_3$ and $Sb_2Te_3$ crystals from 10 K to 270 K, Appl. Phys. Lett. **99**, 261912 (2011).

[35] B. Monserrat, G. J. Conduit, and R. J. Needs, Extracting semiconductor band gap zero-point corrections from experimental data, Phys. Rev. B **90**, 184302 (2014).

[36] J. O. Barnes, J. A. Rayne, and R. W. Ure, Lattice expansion of $Bi_2Te_3$ from 4.2 K to 600 K, Phys. Lett. A **46**, 317 (1974).

[37] J. H. Lloyd-Williams and B. Monserrat, Lattice dynamics and electron-phonon coupling calculations using nondiagonal supercells, Phys. Rev. B **92**, 184301 (2015).

[38] See Supplemental Material at http://link.aps.org/supplemental/10.1103/PhysRevLett.117.226801 for the temperature dependence of the minimum band gaps of $Bi_2Te_3$ and $Sb_2Te_3$.

[39] J. Kim and S.-H. Jhi, Topological phase transitions in group IV-VI semiconductors by phonons, Phys. Rev. B **92**, 125142 (2015).

[40] O. V. Yazyev, E. Kioupakis, J. E. Moore, and S. G. Louie, Quasiparticle effects in the bulk and surface-state bands of

$Bi2Se_3$ and $Bi2Se_3$ topological insulators, Phys. Rev. B **85**, 161101 (2012).

[41] I. Aguilera, C. Friedrich, G. Bihlmayer, and S. Blügel, *GW* study of topological insulators $Bi_2Se_3$, $Bi_2Se_3$, and $Sb_2Te_3$: Beyond the perturbative one-shot approach, Phys. Rev. B **88**, 045206 (2013).

[42] J. Vidal, X. Zhang, L. Yu, J.-W. Luo, and A. Zunger, False-positive and false-negative assignments of topological insulators in density functional theory and hybrids, Phys. Rev. B **84**, 041109 (2011).

[43] W. Li, X.-Y. Wei, J.-X. Zhu, C. S. Ting, and Y. Chen, Pressure-induced topological quantum phase transition in $Sb_2Se_3$, Phys. Rev. B **89**, 035101 (2014).

[44] J. Paier, M. Marsman, K. Hummer, G. Kresse, I. C. Gerber, and J. G. Ángyán, Screened hybrid density functionals applied to solids, J. Chem. Phys. **124**, 154709 (2006).

[45] J. Paier, M. Marsman, K. Hummer, G. Kresse, I. C. Gerber, and J. G. Ángyán, Screened hybrid density functionals applied to solids, J. Chem. Phys. **125**, 249901(E) (2006).

[46] B. M. Wojek, M. H. Berntsen, V. Jonsson, A. Szczerbakow, P. Dziawa, B. J. Kowalski, T. Story, and O. Tjernberg, Direct observation and temperature control of the surface Dirac gap in a topological crystalline insulator, Nat. Commun. **6**, 8463 (2015).

[47] G. Antonius and S. G. Louie, Temperature-induced topological phase transitions: Promoted vs suppressed nontrivial topology, arXiv:1608.00590.